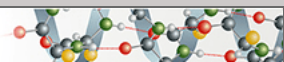


**Protein Structure and Folding:**  
**Crystal Structure of the Human ROR $\alpha$**   
**Ligand Binding Domain in Complex with**  
**Cholesterol Sulfate at 2.2 Å**

PROTEIN STRUCTURE  
AND FOLDING



Joerg Kallen, Jean-Marc Schlaeppli, Francis  
Bitsch, Isabelle Delhon and Brigitte Fournier  
*J. Biol. Chem.* 2004, 279:14033-14038.

doi: 10.1074/jbc.M400302200 originally published online January 13, 2004

---

Access the most updated version of this article at doi: [10.1074/jbc.M400302200](https://doi.org/10.1074/jbc.M400302200)

Find articles, minireviews, Reflections and Classics on similar topics on the [JBC Affinity Sites](https://www.jbc.org/).

Alerts:

- [When this article is cited](#)
- [When a correction for this article is posted](#)

[Click here](#) to choose from all of JBC's e-mail alerts

This article cites 29 references, 7 of which can be accessed free at  
<http://www.jbc.org/content/279/14/14033.full.html#ref-list-1>

# Crystal Structure of the Human ROR $\alpha$ Ligand Binding Domain in Complex with Cholesterol Sulfate at 2.2 Å\*

Received for publication, January 12, 2004  
Published, JBC Papers in Press, January 13, 2004, DOI 10.1074/jbc.M400302200

Joerg Kallen<sup>‡§</sup>, Jean-Marc Schlaeppi<sup>¶</sup>, Francis Bitsch<sup>¶</sup>, Isabelle Delhon<sup>¶</sup>,  
and Brigitte Fournier<sup>¶\*\*</sup>

From the <sup>‡</sup>Discovery Technologies, Protein Structure Unit, the <sup>¶</sup>Discovery Technologies, Biomolecules Production Unit, and the <sup>§</sup>Arthritis and Bone Metabolism, Bone Metabolism Unit, Novartis Pharma AG, CH-4002 Basel, Switzerland

The retinoic acid-related orphan receptor  $\alpha$  (ROR $\alpha$ ) is an orphan member of the subfamily 1 of nuclear hormone receptors. Our recent structural and functional studies have led to the hypothesis that cholesterol or a cholesterol derivative is the natural ligand of ROR $\alpha$ . We have now solved the x-ray crystal structure of the ligand binding domain of ROR $\alpha$  in complex with cholesterol-3-O-sulfate following a ligand exchange experiment. In contrast to the 3-hydroxyl of cholesterol, the 3-O-sulfate group makes additional direct hydrogen bonds with three residues of the ROR $\alpha$  ligand binding domain, namely NH-Gln<sup>289</sup>, NH-Tyr<sup>290</sup>, and NH1-Arg<sup>370</sup>. When compared with the complex with cholesterol, seven well ordered water molecules have been displaced, and the ligand is slightly shifted toward the hydrophilic part of the ligand binding pocket, which is ideally suited for interactions with a sulfate group. These additional ligand-protein interactions result in an increased affinity of cholesterol sulfate when compared with cholesterol, as shown by mass spectrometry analysis done under native conditions and differential scanning calorimetry. Moreover, mutational studies show that the higher binding affinity of cholesterol sulfate translates into an increased transcriptional activity of ROR $\alpha$ . Our findings suggest that cholesterol sulfate could play a crucial role in the regulation of ROR $\alpha$  *in vivo*.

The group of retinoic acid-related orphan nuclear receptors (ROR)<sup>1</sup> is encoded by three different genes ( $\alpha$ ,  $\beta$ , and  $\gamma$ ) (1). ROR $\alpha$  has been implicated in numerous age-related phenotypes such as atherosclerosis, cerebellar atrophy, immunodeficiency, and bone metabolism (2). ROR $\alpha$  was still considered an orphan receptor until we recently reported the first crystal structure of the ROR $\alpha$  LBD. It had revealed a ligand that was unexpectedly present, namely cholesterol (3). We also had shown that the transcriptional activity of ROR $\alpha$  could be mod-

ulated by changes in intracellular cholesterol level or mutation of residues involved in cholesterol binding. This has led to the hypothesis that ROR $\alpha$  could play a key role in the regulation of cholesterol homeostasis and thus represents an important drug target in cholesterol-related diseases. Despite the relatively high homology between ROR $\alpha$  LBD and ROR $\beta$  LBD (63%), cholesterol seems not to be a ligand for the ROR $\beta$  isoform, as reported recently by Stehlin-Gaon *et al.* (4). This indicates a possible distinct function for ROR $\beta$  and ROR $\alpha$ . An inspection of the x-ray structure of the complex between ROR $\alpha$  LBD and cholesterol had shown that in the hydrophilic part of the LBP, there is space for a substituent attached to the hydroxy group of cholesterol, if water molecules are displaced (3). The presence of three arginines (Arg<sup>292</sup>, Arg<sup>370</sup>, and Arg<sup>367</sup>) and of two free backbone amide nitrogens (NH-Gln<sup>289</sup> and NH-Tyr<sup>290</sup>) strongly suggested a negatively charged substituent with at least two hydrogen-bond acceptor functionalities. Docking studies led to the prediction that cholesterol sulfate should have higher affinity than cholesterol, and might be, because of its excellent fit and optimized interactions, the actual natural ligand of ROR $\alpha$  (instead of cholesterol itself). Here, we present the x-ray crystal structure of the ROR $\alpha$  LBD-cholesterol sulfate complex. We show a comparison with the x-ray structure of the ROR $\alpha$  LBD-cholesterol complex, which suggests that cholesterol sulfate has a higher affinity than cholesterol. Indeed, as shown by mass spectrometry analysis, the exchange of cholesterol with cholesterol sulfate is practically irreversible under the conditions used. In addition, DSC analysis revealed that cholesterol sulfate increased the phase transition temperature for ROR $\alpha$  LBD by 9 °C, relative to cholesterol. We also show that cholesterol sulfate shows increased (*versus* cholesterol) transcriptional activation, which is reduced by a point mutation that affects the binding of cholesterol sulfate more than that of cholesterol. We speculate that cholesterol sulfate plays a role in the regulation of ROR $\alpha$  *in vivo*.

## MATERIALS AND METHODS

**ROR $\alpha$  LBD Protein Preparation for Crystallization and ESI-MS Exchange Experiment**—The ROR $\alpha$  LBD protein (residues 271–523, flanked by an N-terminal hexa-His tag and a PreScission<sup>TM</sup> cleavage site) was expressed in the baculovirus system (Sf-9 cells) and purified as described previously (3). The exchange of cholesterol by cholesterol sulfate was done at 37 °C and confirmed by ESI-MS-analysis as reported previously (5). Briefly, cholesterol sulfate was dissolved at 50 mM in Me<sub>2</sub>SO and added at 1.0 mM final concentration to the (His)<sub>6</sub>ROR $\alpha$  LBD<sub>271–523</sub> solution at 73  $\mu$ M. The resulting solution was incubated overnight at 37 °C and further purified by size exclusion chromatography on an SPX75 column before concentration to 17.6 mg/ml for crystallization trials. MS determination of the native complex was done as described previously (5). A control experiment was done by incubating the same amount of ROR $\alpha$  LBD protein with 5% Me<sub>2</sub>SO under identical conditions. The protein concentration was  $\sim$ 15  $\mu$ M in 50 mM AcONH<sub>4</sub>,

\* The costs of publication of this article were defrayed in part by the payment of page charges. This article must therefore be hereby marked "advertisement" in accordance with 18 U.S.C. Section 1734 solely to indicate this fact.

The atomic coordinates and structure factors (code 1SOX) have been deposited in the Protein Data Bank, Research Collaboratory for Structural Bioinformatics, Rutgers University, New Brunswick, NJ (<http://www.rcsb.org/>).

§ To whom correspondence may be addressed. E-mail: joerg.kallen@pharma.novartis.com.

\*\* To whom correspondence may be addressed. E-mail: brigitte.fournier@pharma.novartis.com.

<sup>1</sup> The abbreviations used are: ROR, retinoic acid-related orphan nuclear receptor; LBD, ligand binding domain; LBP, ligand binding pocket; ESI-MS, electrospray ionization mass spectrometry; DSC, differential scanning calorimetry.

pH 7.0. Both spectra were recorded under identical conditions with  $V_c = 20$  volts.

**Differential Scanning Calorimetry**—The ROR $\alpha$  LBD complexes with cholesterol and cholesterol sulfate, respectively, were obtained as described above. After the exchange experiment, the excess of cholesterol sulfate was removed on 5-ml HiTrap desalting columns. Protein concentration was determined by high pressure liquid chromatography-UV detection (214 nm). The final protein concentration following ligand exchange was 20  $\mu$ M. DSC scans were obtained using a MicroCal VP-capDSC system (MicroCal, LLC, Northampton, MA) at a scan rate of 250  $^{\circ}$ C/h.

**Crystallization, Data Collection, and Structure Determination**—Crystals were obtained at 4  $^{\circ}$ C by the vapor diffusion method in 2- $\mu$ l hanging drops containing equal volumes of protein (17.6 mg/ml) and crystallization buffer (0.2 M  $MgCl_2$ , 16% w/v polyethylene glycol 4000, 0.1 M Tris HCl, pH 8.5). The crystal form obtained was similar to the one for the complex with cholesterol (3). Diffraction data at 100 K were collected at the Swiss Light Source (beamline X06SA) using a Marresearch CCD detector and an incident monochromatic x-ray beam with 0.9200- $\text{\AA}$  wavelength. In total, 226 images were collected with 1.0 $^{\circ}$  rotation each, using an exposure time of 9 s/frame and a crystal-to-detector distance of 150 mm. Raw diffraction data were processed and scaled with the HKL program suite version 1.96.1 (6). The estimated  $B$ -factor by Wilson plot analysis is 32.9  $\text{\AA}^2$ . The structure was determined using as starting model the coordinates of the complex ROR $\alpha$  LBD-cholesterol refined to 1.63- $\text{\AA}$  resolution (3). The program REFMAC version 5.0 (7, 8) was used for refinement. Bulk solvent correction, an initial anisotropic  $B$  factor correction, and restrained isotropic atomic  $B$ -factor refinement were applied. The refinement target was the maximum likelihood target using amplitudes. No  $\sigma$  cut-off was applied on the structure factor amplitudes. Cross-validation was used throughout refinement using a test set comprising 5.0% (829) of the unique reflections. Water molecules were identified with the program ARP/wARP (7, 9) and selected based on difference peak height (greater than 3.0  $\sigma$ ) and distance criteria. Water molecules with temperature factors greater than 70  $\text{\AA}^2$  were rejected. The program O version 7.0 (10) was used for model rebuilding, and the quality of the final refined model was assessed with the programs PROCHECK version 3.3 (11) and REFMAC version 5.0 (7, 8). Crystal data, data collection, and refinement statistics are shown in Table I.

**Reagents, Plasmids and Mutations for Transcriptional Activity Assays**—The COS-7 cells (ATCC, Manassas, VA, CRL1651) and the human osteosarcoma cell line, U-2OS, (ATCC, Crl HTB 96) were purchased from ATCC. Cholesterol and cholesterol sulfate were purchased from Steraloids (Newport, RI). The pCMX-ROR $\alpha$  plasmid was a kind gift from Dr. M. Becker-Andre (Serono, Geneva, Switzerland). The reporter ROREtkluc was a kind gift from Dr. V. Giguere (McGill Univ, Montreal, Canada) and has been described previously (12). The ROR $\alpha$  mutants C228Q, A330Q, A371Q, C323L, and K339A, E509A were generated using a QuikChange XL site-directed mutagenesis kit from Stratagene (La Jolla, CA).

**Cell Culture and Transfection Assays**—Cells were seeded in 12-well plates at a density of  $1 \times 10^5$  cells/cm $^2$ , 24 h before transfection, and transfected using Eugene6 transfection reagent (Roche Applied Science). A typical reaction mixture contained 0.5  $\mu$ g pCMX-ROR $\alpha$  expression vector, 1.0  $\mu$ g of reporter plasmid ROREtkluc, 0.1  $\mu$ g of pCMV- $\beta$ -galactosidase, and 3  $\mu$ l of Eugene 6. After a 4-h exposure to the transfection mix, the medium was refreshed and left for another 24 h. Transfected cells were subsequently harvested for the luciferase assay by scraping the cells into 250  $\mu$ l of passive lysis buffer after washing them in phosphate-buffered saline. Luciferase activity was monitored according to the Promega luciferase assay kit using an automatic luminometer LB96P (Berthold, Regensburg, Germany). Results are expressed in relative light units per  $\beta$ -galactosidase unit.

## RESULTS AND DISCUSSION

**Structure Determination of the Complex ROR $\alpha$  LBD-Cholesterol Sulfate**—We have expressed human ROR $\alpha$  LBD (residues 271–523, numbering according to splice variant 1 of SWISS-PROT entry P35398, and a PreScission<sup>TM</sup> cleavable N-terminal His tag) in the baculovirus system. After a two-step purification and without cleaving off the N-terminal tag, we exchanged to more than 95% bound cholesterol with cholesterol sulfate (as determined by ESI-MS analysis) and crystallized the complex. Crystals belonging to the monoclinic space group  $P2_1$  (unit cell:  $a = 54.4$   $\text{\AA}$ ,  $b = 49.9$   $\text{\AA}$ ,  $c = 60.7$   $\text{\AA}$ ,  $\beta = 97.8^{\circ}$ , 1 complex/

TABLE I  
Crystallographic summary

Diffraction data	
Space group	$P2_1$
Unit cell dimensions	$a = 54.4$ $\text{\AA}$ $b = 49.9$ $\text{\AA}$ $c = 60.7$ $\text{\AA}$ $\beta = 97.8^{\circ}$
Resolution range	20.0–2.2 $\text{\AA}$ (2.28–2.20 $\text{\AA}$ )
No. of observations	57,993
No. of unique reflections	16,541
$\langle I/\sigma(I) \rangle$	16.2
$R_{\text{sym}}$ on intensities <sup>a</sup>	0.079
Completeness	99.7% (99.4%)
Refinement	
Resolution range	20.0–2.20 $\text{\AA}$
$R_{\text{cryst}}$ <sup>b</sup>	0.194
$R_{\text{free}}$	0.219
Protein atoms	2,067
Ligand atoms	33
Solvent atoms	255
Average $B$ -factor	40.0 $\text{\AA}^2$
r.m.s.d. <sup>c</sup> from target values	
Bond lengths	0.014 $\text{\AA}$
Bond angles	1.41 $^{\circ}$

$$^a R_{\text{sym}} = \sum I_{\text{avg}} - I_i / \sum I_i$$

<sup>b</sup>  $R_{\text{cryst}} = \sum F_o - F_{\text{calc}} / \sum F_o$ , where  $F_o$  and  $F_{\text{calc}}$  are observed and calculated structure factors,  $R_{\text{free}}$  is calculated for a randomly chosen 5% of reflections, and  $R_{\text{cryst}}$  is calculated for the remaining 95% of reflections.

<sup>c</sup> r.m.s.d., root mean square deviation.

asymmetric unit) reached maximal dimensions of up to 0.2 mm in hanging drops at 4  $^{\circ}$ C within 6 weeks. The structure was solved using the coordinates of the complex of ROR $\alpha$  LBD with cholesterol (3).

**Overall Structure of the Complex ROR $\alpha$  LBD-Cholesterol Sulfate**—The results of the crystallographic refinement are summarized in Table I. The nomenclature of the secondary structure elements is based on the RXR LBD crystal structure (13) and is identical to the one used for ROR $\alpha$  LBD (3). In general, the electron density is of excellent quality, except for amino acids 461–466 (loop L9–10), which had only weak density. The protein part of the refined model consists of the last two His amino acids from the His tag followed by the PreScission<sup>TM</sup> site (LEVLFQG) and by amino acids 271–511 of the ROR $\alpha$  LBD. The refined model also contains 256 water molecules and one cholesterol sulfate molecule. ROR $\alpha$  LBD bound to cholesterol sulfate is in an agonist-bound state, as judged by the position of H12 (14). H12 in this position, together with the H3-H4 region, forms the interaction surface (AF-2) for the coactivator (14). As found previously for the complex with cholesterol (3), the PreScission<sup>TM</sup> cleavage site (LEVLFQGP) acts as a mimic of the LXXLL coactivator sequence and adopts an  $\alpha$ -helical conformation. It interacts with the coactivator binding site of a neighboring molecule in the crystal lattice and forms the classical “charge clamp” capping interactions mediated by Lys<sup>339</sup>(H3) and Glu<sup>509</sup>(H12). The overall structures of ROR $\alpha$  LBD in complex with cholesterol and cholesterol sulfate are very similar. The root mean square deviation using the LSQ option from the program O (10) was 0.26  $\text{\AA}$  for the 242 C $\alpha$  atoms from residues Pro<sup>270</sup>-Phe<sup>511</sup>. Significant changes in the protein parts of the LBP (Fig. 1A) occur only for the side chain of Ile<sup>327</sup> and the loop L1–2 (residues Gln<sup>289</sup> and Tyr<sup>290</sup>). The backbone NH-atoms for Gln<sup>289</sup> and Tyr<sup>290</sup> move by ca. 0.8  $\text{\AA}$  toward the sulfate group (with a concomitant movement of the respective side chains), thus improving the interactions with the sulfate group. The side chain of Ile<sup>327</sup> has moved slightly, to prevent a steric clash with the terminal isopropyl group of cholesterol sulfate.

**Cholesterol Sulfate in the LBP of ROR $\alpha$** —Cholesterol sulfate is bound in the LBP of ROR $\alpha$ . The sulfate group, which is



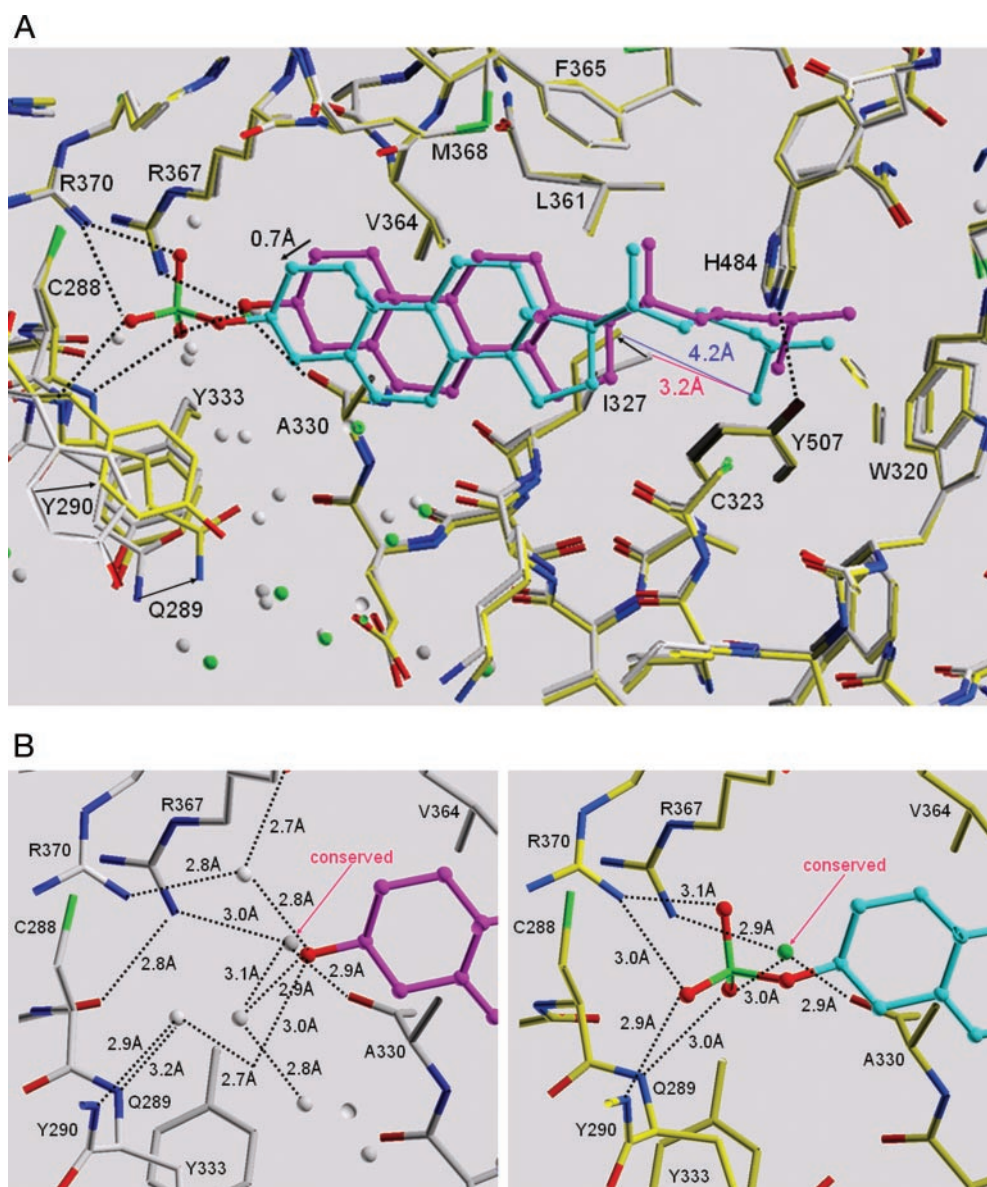


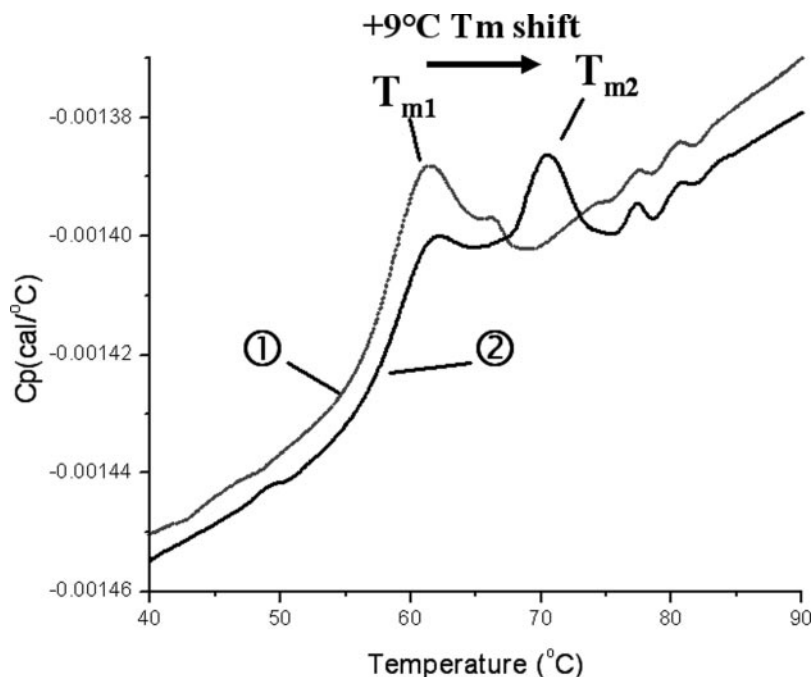
**FIG. 1. Crystal structure of the complex between human ROR $\alpha$  LBD and cholesterol sulfate.** *A*, an overview of the interactions made by cholesterol sulfate (cyan) with the LBP of ROR $\alpha$  LBD (yellow). Selected hydrogen bonds are shown as dotted lines. The sulfate group makes direct hydrogen bonds with NH-Gln<sup>289</sup>, NH-Tyr<sup>290</sup>, NH1-Arg<sup>370</sup>, and a water-mediated hydrogen bond with NH1-Arg<sup>367</sup>. Also shown is a superposition with the x-ray structure of ROR $\alpha$  LBD-cholesterol (whitel/magenta). Water molecules for the complexes with cholesterol sulfate and cholesterol are shown as green and white spheres, respectively. Only the regions comprising Gln<sup>289</sup>, Tyr<sup>290</sup> (loop L1–2), and Ile<sup>327</sup> show significant changes (black arrows). Gln<sup>289</sup> and Tyr<sup>290</sup> move toward the sulfate group to improve the interactions of their main chain NH-moieties with the sulfate group. CD1-Ile<sup>327</sup> has moved to avoid a steric clash (red line, 3.2 Å) with the isopropyl group of cholesterol sulfate (true distance is 4.2 Å, blue line). *B*, a comparison of ROR $\alpha$  LBD/cholesterol (left) and ROR $\alpha$  LBD/cholesterol sulfate (right) in the hydrophilic part of the corresponding LBPs. Selected hydrogen bonds are shown as dotted lines. Seven well ordered water molecules (six of which are shown as gray spheres) present for cholesterol (left) have been displaced in the complex with cholesterol sulfate (right). Only one conserved water molecule (red arrow) is still present that mediates interactions between the sulfate group and NH1-Arg<sup>367</sup> and O-Ala<sup>330</sup>. The sulfate group makes direct hydrogen bond interactions with NH-Gln<sup>289</sup>, NH-Tyr<sup>290</sup>, and NH1-Arg<sup>370</sup>.

located in the hydrophilic part of the LBP, makes direct hydrogen bond interactions with NH-Gln<sup>289</sup> (3.0 Å), NH-Tyr<sup>290</sup> (2.9 Å), and a bidentate interaction with NH1-Arg<sup>370</sup> (3.0 Å, 3.1 Å). This confirms the docking hypothesis, which had led to the proposal of cholesterol sulfate as a ligand with an improved affinity relative to cholesterol (3). In addition, a water-mediated interaction is made with NH1-Arg<sup>367</sup> (Fig. 1A). The comparison shows that cholesterol sulfate and cholesterol have a similar overall mode of binding, but cholesterol sulfate is displaced slightly toward the hydrophilic and positively charged part of the LBP (Fig. 1A). This can be explained by the optimization of electrostatic and hydrogen-bond interactions made by the sulfate group. Interestingly, seven well ordered water mol-

ecules present for cholesterol in the hydrophilic part of the LBP have been displaced in the complex with cholesterol sulfate (Fig. 1B). Only one conserved water molecule is still present, which mediates interactions from the sulfate group to NH1-Arg<sup>367</sup> and O-Ala<sup>330</sup>.

The average *B*-value for the ligand (28.7 Å<sup>2</sup>) is lower than the average *B*-value for the protein (40.0 Å<sup>2</sup>), consistent with the fact that excellent electron density for all non-hydrogen atoms of cholesterol sulfate is visible. Cholesterol sulfate adopts thus (like cholesterol) a single, well defined position in the LBP. The following amino acids have a non-hydrogen atom closer than 4 Å to the ligand cholesterol sulfate: Cys<sup>288</sup> (loop H1-H2), Gln<sup>289</sup> (loop H1-H2), Tyr<sup>290</sup> (loop H1-H2), Trp<sup>320</sup> (H3), Cys<sup>323</sup>.

FIG. 2. Cholesterol sulfate has a higher affinity than cholesterol for ROR $\alpha$  LBD, as confirmed by differential scanning calorimetry. DSC scans of ROR $\alpha$  LBD complex with cholesterol (dotted line, curve 1;  $T_{m1}$  = 61.6 °C) and ROR $\alpha$  LBD complex with cholesterol sulfate (solid line, curve 2;  $T_{m2}$  = 70.6 °C) are shown. The shoulder around 62 °C for curve 2 is due to a remaining fraction of non-exchanged cholesterol. Temperature scan rate was 250 °C/h, and protein concentration was 20  $\mu$ M. The +9 °C  $T_m$  shift indicates a higher stability for the complex with cholesterol sulfate.



(H3), Ala<sup>324</sup>(H3), Lys<sup>326</sup>(H3), Ile<sup>327</sup>(H3), Ala<sup>330</sup>(H3), Val<sup>364</sup>-(H5), Arg<sup>367</sup>(H5), Met<sup>368</sup>(H5), Arg<sup>370</sup>(H5), Ala<sup>371</sup>(H5), Val<sup>379</sup>-(s1), Tyr<sup>380</sup>(s1), Phe<sup>381</sup>(s1), Phe<sup>391</sup>(H6), Leu<sup>394</sup>(H6), Val<sup>403</sup>(H7), and His<sup>484</sup>(H11).

**Cholesterol Sulfate Is Bound More Tightly than Cholesterol**—We used non-denaturing ESI-MS to confirm the exchange of cholesterol by cholesterol sulfate in the ROR $\alpha$  LBD. Exchange yield using cholesterol sulfate was greater than 95%. As shown previously (5), the corresponding protein-ligand complex also showed a higher stability to collision-induced dissociation in the electrospray ionization interface. Moreover, the exchange of bound cholesterol sulfate could not be reversed by adding back an excess of cholesterol or other cholesterol derivatives such as hydroxycholesterols (data not shown). In addition, differential scanning calorimetry was used to assess the stabilities of the ROR $\alpha$  LBD complexes with cholesterol and cholesterol sulfate, respectively. Fig. 2 shows that cholesterol sulfate dramatically increased the phase transition temperature of ROR $\alpha$  LBD by 9 °C, relative to cholesterol. Overall, these results confirm that, as predicted by the x-ray structures, cholesterol sulfate has a higher affinity than cholesterol for ROR $\alpha$  LBD.

**Sulfonation of Cholesterol Improves ROR $\alpha$  Transcriptional Activity**—To further characterize the possible biological role of cholesterol sulfate for ROR $\alpha$ , a series of mutations was designed and evaluated for their effects on the transcriptional activities. The double mutation K339A,E509A (*i.e.* a “knockout” of the charge clamp) was made as a negative control. Indeed, this double mutant triggered a transcriptional activity similar to the one obtained with an empty vector (Fig. 3A). The triple mutant A330Q,A371Q,C323L (designed to prevent binding of cholesterol and cholesterol sulfate in the LBP) showed a reduced activity (Fig. 3A) consistent with the results obtained previously for the single mutants A330L, A371Q, and C323L (3). A mutation that might prevent binding of cholesterol sulfate more than that of cholesterol was designed based on the crystal structure. We hypothesized that the mutation C288Q would modify the position of Arg<sup>370</sup> and/or of loop L1–2 (Fig. 1B) and thus would preferentially lower the affinity of cholesterol sulfate *versus* cholesterol. We first tested this mutation in cells for which the intracellular cholesterol level was not ma-

nipulated. Most likely, as shown in normal epithelial cells, the ratio between cholesterol and cholesterol sulfate in these cells is about 500:1 (15). Under these experimental conditions, the transcriptional activity of the mutant ROR $\alpha$  C288Q was found to be similar to the one elicited by ROR $\alpha$  wild type (Fig. 3A). This unaffected transcriptional activity of the C288Q mutant probably reflects the binding of cholesterol to the mutated ROR $\alpha$ .

The intracellular cholesterol level in U2OS cells can be reduced by using lovastatin (hydroxymethylglutaryl-CoA reductase inhibitor) and cyclodextrin, as described previously (3). Under these conditions, using ROR $\alpha$  wild type, we have shown that cholesterol sulfate elicited an increased transcriptional activity of 160% when compared with cholesterol. In contrast, the mutant C288Q did not display this improved transcriptional activity (with respect to cholesterol) when cells were treated with cholesterol sulfate (Fig. 3B). This is consistent with the prediction that the C288Q mutant preferentially reduces the affinity of cholesterol sulfate. We cannot exclude that the only partial cholesterol depletion in these cells might reduce this observed effect on cholesterol sulfate. It would be interesting to investigate ROR $\alpha$  transcriptional activity in cells for which the cholesterol:cholesterol sulfate ratio is more drastically modified such as in keratinocytes during differentiation, where this ratio is as low as 5:1, or in ichthyosis-derived cells, where this ratio is even further reduced to 1:1 (16, 17).

Recently, there has been an increasing interest in steroid sulfonation, in particular for their potential involvement in breast and prostate cancer (18). It is postulated that estrone sulfate in the breast tumors (19) could play a role in regulating the level and the activity of 17 $\beta$ -estradiol and that disruption of estrogen sulfotransferase could lead to modulation of the estrogen pathway (20). In our study, we show that sulfonation of cholesterol allows improved binding to ROR $\alpha$ , reflected by an increased transcriptional activity. The possible exchange of cholesterol with cholesterol sulfate inside the cells could represent a mode of regulation of intracellular cholesterol level since it has been shown that cholesterol sulfate inhibits cholesterol esterification (21) and that cholesterol sulfate could potentially modulate hydroxymethylglutaryl-CoA, the rate-limiting enzyme for cholesterol synthesis (22). The identification of

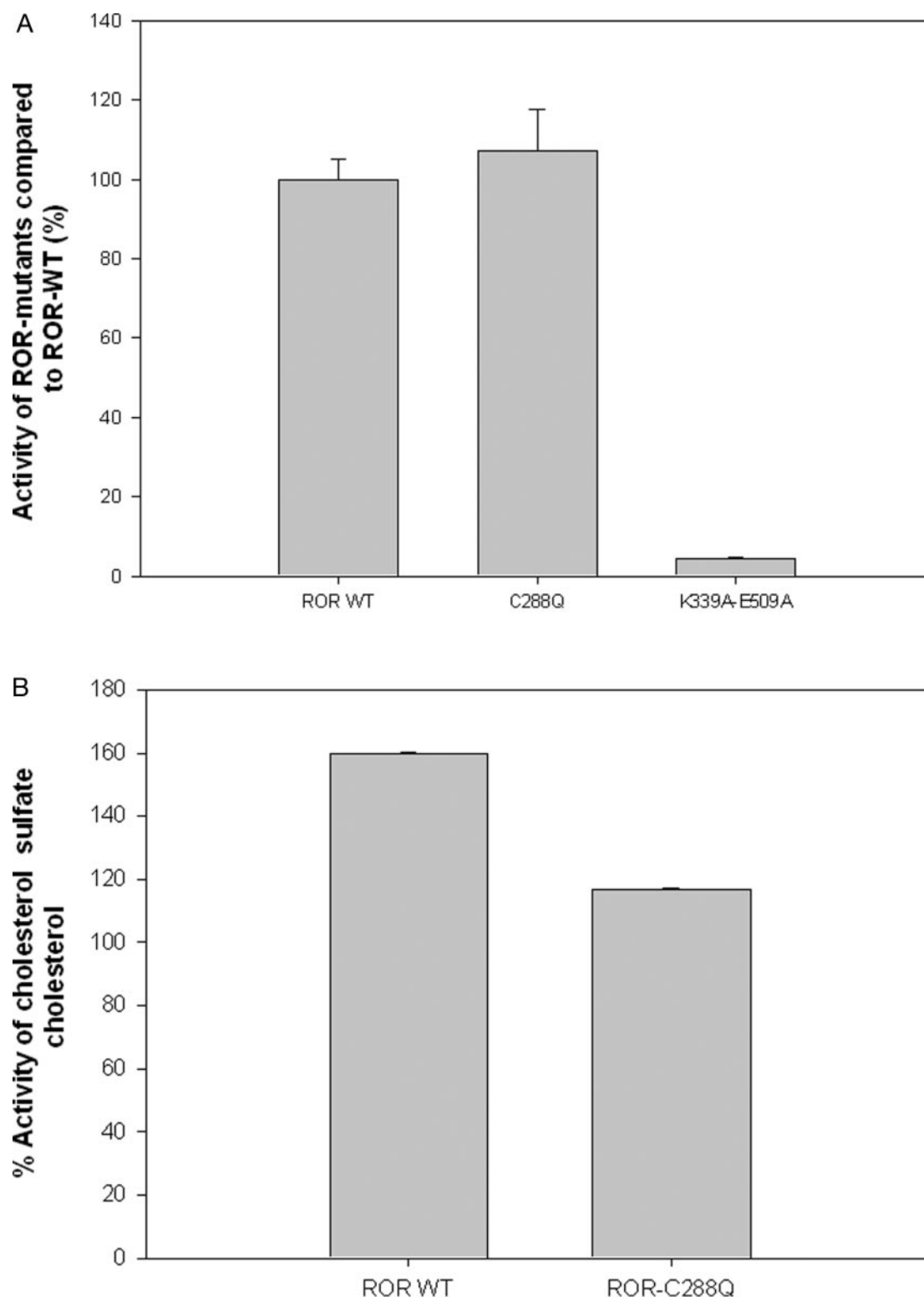


**FIG. 3. Effect of ROR $\alpha$  mutations on transcriptional activities induced by cholesterol sulfate or cholesterol.** A, transcriptional activity of ROR $\alpha$  wild type (WT) and mutants. Cos7 cells were seeded at a density of  $1 \times 10^5$  cells/cm<sup>2</sup> in 12-well plates and transiently transfected with 0.50  $\mu$ g of expression vector for ROR $\alpha$  wild type or ROR $\alpha$  mutants (C288Q and K339A,E509A) together with 1.0  $\mu$ g of ROREtkluc and as indicated under "Materials and Methods." 24 h after transfection, cells were collected with 250  $\mu$ l of passive lysis buffer, and luciferase activity was determined in duplicate on 20  $\mu$ l of cell extracts. Luminescence data were corrected with  $\beta$ -galactosidase activity and expressed as relative luminescence unit/ $\beta$ -galactosidase unit. Results are expressed as percentage of induction when compared with the activity of wild type ROR $\alpha$ . Western blot analysis of extracts from cells transfected was performed and showed comparable expression of ROR $\alpha$  wild type and mutants (data not shown). B, U2OS cells were transfected as described under "Materials and Methods" with ROR $\alpha$  wild type and ROR $\alpha$  C288Q. After transfection, cells were treated with hydroxypropylcyclodextrin (10 mM) in presence of 5  $\mu$ M lovastatin for 4 h in a medium containing 10% low density lipoprotein-free serum. After four h, the medium was removed, and cells were treated with vehicle (ethanol or Me<sub>2</sub>SO) or cholesterol or cholesterol sulfate at 10  $\mu$ M in presence of 5  $\mu$ M lovastatin. Twenty-four hours after transfection, cells were collected with 250  $\mu$ l of passive lysis buffer, and luciferase activity was determined in duplicate on 20  $\mu$ l of cell extract from three separate culture dishes. Luminescence data were corrected with  $\beta$ -galactosidase activity and expressed as relative luminescence unit/ $\beta$ -galactosidase unit. Results are expressed as the percentage of induction of cholesterol sulfate when compared with cholesterol for ROR $\alpha$  and ROR $\alpha$  C288Q.

ROR $\alpha$  target genes possibly involved in these mechanisms could contribute to a better understanding of these regulations by cholesterol sulfate.

Despite the fact that cholesterol sulfate is widely distributed in human tissues, its physiological role is not well understood (for a review, see Ref. 23). In skin, an important role for cholesterol sulfate emerged, *e.g.* in recessive X-linked ichthyosis for which a genetic deficiency in steroid sulfatase leads to the accumulation of cholesterol sulfate in stratum corneum (16). In addition, the role of cholesterol sulfate in keratinocyte differentiation has been well documented (24–27). It would therefore be interesting to reconsider ROR $\alpha$  function in organs such as skin and testis, in which cholesterol sulfate was found to be abundant and which display the strongest expression of ROR $\alpha$  (28).

In addition, cholesterol sulfate is also a possible precursor of important sulfonated adrenal steroids such as dehydroepiandrosterone sulfate and pregnenolone sulfate (23, 29). It is worth noting that pregnenolone sulfate, now considered as an essential neurosteroid, is actively synthesized in brain, in particular in Purkinje cells (30). This information could thus also shed new light on the well described cerebellar phenotype of the ROR $\alpha$  mutant mice (31).

**Acknowledgments**—We thank Drs. M. Geiser and S. Geisse for cloning and fermentation and R. Cebe, Y. Pouliquen, A. Berner, and A. Graham for technical assistance. The use of the Novartis modeling software WITNOTP, written by A. Widmer, and the experimental assistance from the Swiss Light Source (PX Beam Line X06SA), C. Schulze-Bries, is acknowledged. We thank H. Widmer, H. P. Kocher, R. Gamse, and M. Missbach for interest and support.

#### REFERENCES

1. Jetten, A. M., Kurebayashi, S., and Ueda, E. (2001) *Prog. Nucleic Acid Res. Mol. Biol.* **69**, 205–247
2. Jarvis, C. I., Staels, B., Brugg, B., Lemaigre-Dubreuil, Y., Tedgui, A., and Mariani, J. (2002) *Mol. Cell. Endocrinol.* **186**, 1–5
3. Kallen, J., Schlaeppli, J.-M., Bitsch, F., Geisse, S., Geiser, M., Delhon, I., and Fournier, B. (2002) *Structure* **10**, 1697–1707
4. Stehlin-Gaon, C., Willmann, D., Zeyer, D., Sanglier, S., Van Dorsselaer, A., Renaud, J.-P., Moras, D., and Schüle, R. (2003) *Nat. Struct. Biol.* **10**, 820–825
5. Bitsch, F., Aichholz, R., Kallen, J., Geisse, S., Fournier, B., and Schlaeppli, J.-M. (2003) *Anal. Biochem.* **323**, 139–149
6. Otwinowski, Z., and Minor, W. (1997) *Methods Enzymol.* **276**, 307–326
7. Collaborative Computational Project, Number 4 (1994) *Acta Crystallogr. Sect. D Biol. Crystallogr.* **50**, 760–763
8. Murshudov, G. N., Vagin, A. A., and Dodson, E. J. (1997) *Acta Crystallogr. Sect. D Biol. Crystallogr.* **53**, 240–255
9. Lamzin, V. S., Perrakis, A., and Wilson, K. S. (2001) in *International Tables for Crystallography* (M. G. Rossmann and E. Arnold, eds) Vol. F, pp. 720–722, Kluwer Academic Publishers, Norwell, MA
10. Jones, T. A., Zou, J. Y., Cowan, S. W., and Kjeldgaard, M. (1991) *Acta Crystallogr. Sect. A* **47**, 110–119
11. Laskowski, R. A., MacArthur, M. W., Moss, D. S., and Thornton, J. M. (1993) *J. Appl. Cryst.* **26**, 283–291
12. Giguere, V., Tini, M., Flock, G., Ong, E., Evans, R. M., and Otulakowski, G. (1994) *Genes Dev.* **8**, 538–553
13. Bourguet, W., Ruff, M., Chambon, P., Gronemeyer, H., and Moras, D. (1995) *Nature* **375**, 377–382
14. Renaud, J. P., and Moras, D. (2000) *Cell. Mol. Life Sci.* **57**, 1748–1769
15. Lin, Y. N., and Horowitz, M. I. (1980) *Steroids* **36**, 697–708
16. Epstein, E. H., Jr., Krauss, R. M., and Shackleton, C. H. (1981) *Science* **214**, 659–660
17. Williams, M. L., and Elias, P. M. (1981) *J. Clin. Invest.* **68**, 1404–1410
18. Strott, C. A. (2002) *Endocr. Rev.* **23**, 703–732
19. Falany, J., Macrina, N., and Falany, C. N. (2002) *Breast Cancer Res. Treat.* **74**, 167–176
20. Qian, Y. M., Sun, X. J., Tong, X. P., Li, P., Richa, J., and Song, W. C. (2001) *Endocrinology* **142**, 5342–5350
21. Nagakawa, M., and Kojima, S. (1976) *J. Biochem. (Tokyo)* **80**, 729–733
22. Williams, M. L., Hugues-Fulford, M., and Elias, P. M. (1985) *Biochim. Biophys. Acta* **854**, 349–357
23. Strott, C. A., and Higashi, Y. (2003) *J. Lipid Res.* **44**, 1268–1278
24. Hanley, K., Wood, L., Ng, D. C., He, S. S., Lau, P., Moser, A., Elias, P. M., Bikle, D. D., Williams, M. L., and Feingold, K. R. (2001) *J. Lipid Res.* **42**, 390–398
25. Jetten, A. M., George, M. A., Nervi, C., Boonen, L. R., and Rearick, J. F. (1989) *J. Invest. Dermatol.* **92**, 203–209
26. Kawabe, S., Ikuta, T., Ohba, M., Chida, K., Ueda, K., Yamanishi, K., and Kuroki, T. (1998) *J. Invest. Dermatol.* **111**, 1098–1102
27. Kashiwagi, M., Ohba, M., Chida, K., and Kuroki, T. (2002) *J. Biochem. (Tokyo)* **132**, 853–857
28. Steinmayr, M., Andre, E., Conquet, F., Rondi-Reig, L., Delhaye-Bouchaud, N., Auclair, N., Daniel, H., Crepel, F., Mariani, J., Sotelo, C., and Becker-Andre, M. (1998) *Proc. Natl. Acad. Sci. U. S. A.* **95**, 3960–3965
29. Mason, J. I., and Hemsell, P. G. (1982) *Endocrinology* **111**, 208–213
30. Tsutui, K., Sakamoto, H., and Ukena, K. (2003) *J. Steroid Biochem. Mol. Biol.* **85**, 311–321
31. Hamilton, B. A., Frankel, W. N., Kerrebrock, A. W., Hawkins, T. L., FitzHugh W., Kusumi, K., Russell, Mueller, K. L., van Berkel, V., Birren, B. W., Kruglyak, L., and Lander, E. S. (1996) *Nature* **379**, 736–739